Understanding the behaviour of different metals in loaded scintillators: discrepancy between gadolinium and bismuth

Guillaume H. V. Bertrand, Jonathan Dumazert, Fabien Sguerra, Romain Coulon, Gwenolé Corre, Matthieu Hamel

Understanding the behavior of different metals in loaded scintillators: discrepancy between gadolinium and bismuth

Guillaume H.V. Bertrand, Jonathan Dumazert, Fabien Sguerra, Romain Coulon, Gwenolé Corre and Matthieu Hamel*

CEA, LIST, Laboratoire Capteurs et Architectures Électroniques, F-91191 Gif-sur-Yvette, France.

*Corresponding author: Matthieu Hamel, Laboratoire Capteurs & Architectures Électroniques, DRT/LIST/DM2I/LCAE

CEA Saclay

91191 Gif Sur Yvette Cedex

Phone: +33 (0)169083325

email: matthieu.hamel@cea.fr (please do not send commercial emails)

Keywords: Plastic scintillator, bismuth loading, gadolinium loading, gamma spectrometry, thermal neutron detection

ABSTRACT: Organometallic chemistry has recently gained a lot of attention in the domain of plastic scintillators. Homogenously dispersed metal complex in a polymer matrix can afford plastic scintillators with unseen ability. Heavy atom loading is very attractive as it gives us access to plastics with increased sensitivity towards elusive radiation such as gamma and neutrons. But this comes with a drawback, as heavy atoms tend to quench fluorescence, hence decreasing the scintillation yield. We present here a comprehensive study of this phenomenon with bismuth and gadolinium complexes. We investigate the influence of the ligands nature by varying organometallics and fluorophore concentration to probe their interaction. We also propose an explanation of the difference of behavior between these two complexes. These results were applied to the fabrication of large volume loaded plastic scintillators (> 100 cm^3). Bismuth loaded scintillator displayed characteristics on par with commercial equivalent and gadolinium one proved to be able to detect thermal neutrons.

Introduction

Following recent events, homeland security is more than ever a preoccupation for government and intergovernmental agencies. In this context, radiological and nuclear safety is a priority as it is mandatory to compartmentalize radioactive materials from civil world. To achieve this goal a large scale deployment of detectors is necessary to monitor the flow of people and goods. Plastic scintillator (PS) is the cheapest and most accessible solution[1] as opposed to inorganic scintillators, NaI(Tl), CZT or HPGe technologies.[2] But, as nothing is perfect, PS technology presents certain drawbacks such as poor sensitivity towards gamma and neutron radiations and poor energy resolution.[3]

After almost twenty years of inactivity, the last decade has seen major breakthroughs in the modification of plastic scintillators in order to tackle those issues and improve their overall characteristics.[1] For example high concentration of fluorophore successfully performed efficient neutron/gamma discrimination which was considered un-achievable years before.[4] A major field of research is the incorporation of various elements in PS, as it is an elegant and versatile solution to PSs' drawbacks. Different strategies can be imagined to add an element to the PS composition, but the use of organometallics is proving to be the most promising in term of process, flexibility and performances. As an example the use of iridium(III) complex as a triplet harvester and fluorophore is extensively researched to obtain high scintillation yields.[5,6]

Fluoride[7], tin[8], lead[9–13] and bismuth[14,15] were used to achieve high density and X-ray / low energy gamma spectrometry. Lithium (^{6}Li)[16,17], boron (^{10}B)[18–21] and gadolinium[22,23] were employed for thermal neutron detection due to their high thermal cross-section.

As most recent studies showed, Bi[24,25] and Gd[26,27] are leaders in their field, respectively increased density and neutrons detection. However their incorporation in PS always comes with the tradeoff of lower scintillation yields.

We present here a protocol for improved bismuth and gadolinium-loaded PS and their characteristics. In order to understand the mechanism behind fluorescence quenching due to heavy atoms we explored the influence of metal versus fluorophore loading on the scintillation yields. As an application of our optimization large scale loaded PSs (> 100 cm^3) were synthesized and characterized.

Experimental section

Solvents were purchased from VWR; reagents were purchased from Sigma-Aldrich excepted triphenyl bismuth which was acquired from PHDS and gadolinium tristetramethylheptanedionate which was acquired from Strem chemicals. Monomers were distilled over CaH_2 under reduced pressure to get rid of inhibitors and impurities. Other reagents were used without further purifications.

General procedure for plastic scintillator preparation

Desired solids (fluorescent dyes and bismuth/gadolinium complexes) and monomers were inserted in a suitable round bottom flask. Quantities were previously calculated regarding the desired final composition. The resulting solution was put under a nitrogen atmosphere then frozen using liquid nitrogen and multiple freeze–pump–thaw cycles were performed to achieve total degassing. This was poured into a cylindrical glass mold containing a small quantity of initiator. The filed mold was then purged with nitrogen, sealed and placed into an oven at 40/45°C for 15 to 30 days (bismuth) or 60°C for 10 to 15 days (gadolinium). When total polymerization was observed the mold was cooled down to room temperature and then shattered to free the plastic piece. The cylindrical samples were shaped, polished and, if desired, covered with a reflecting paint for the scintillation experiment.

Bismuth loaded plastic scintillator and gadolinium loaded plastic scintillators compositions are respectively given in Table 1 and Table 2.

Table 1 composition of PSs with varying amount of $BiPh_3$ and 2,5-diphenyloxazole (PPO). 1,4-Bis(2-methylstyryl)benzene (Bis-MSB) amount was kept to 0.9 mg in each sample.

	$V_{styrene}$ (mL)	$V_{curing\ agent}$ (mL)	m_{BiPh3} (mg)	m_{PPO} (mg)
A1	2.46	0.74	0	15
A2	2.41	0.72	70	15
A3	2.36	0.71	130	15
A4	2.17	0.65	360	15
A5	1.79	0.54	820	15
B1	2.45	0.74	0	30
B2	2.39	0.72	70	30
B3	2.34	0.70	130	30
B4	2.15	0.65	360	30
B5	1.77	0.53	820	30
C1	2.40	0.72	0	90
C2	2.34	0.70	70	90
C3	2.29	0.69	130	89
C4	2.11	0.63	360	80
C5	1.75	0.52	820	60
D1	2.24	0.67	0	280
D2	2.19	0.66	70	275
D3	2.15	0.65	130	265
D4	1.97	0.59	360	250
D5	1.60	0.48	820	240
E1	1.91	0.57	0	690
E2	1.85	0.55	70	690
E3	1.82	0.55	130	660
E4	1.66	0.50	360	630
E5	1.30	0.39	820	600

Table 2 composition of PSs with varying amount of $Gd(TMHD)_3$ and PPO. Bis-MSB amount was kept to 0.9 mg in each sample.

	$V_{styrene}$ (mL)	$V_{curing\ agent}$ (mL)	$m_{Gd(TMHD)3}$ (mg)	m_{PPO} (mg)
F1	2,46	0,74	0	15
F2	2,34	0,70	150	15
F3	2,22	0,67	290	15
F4	1,74	0,52	875	13
G1	2,45	0,74	0	30
G2	2,33	0,70	150	30
G3	2,21	0,66	290	30
G4	1,73	0,52	875	30
H1	2,40	0,72	0	90
H2	2,28	0,68	150	90
H3	2,17	0,65	290	85
H4	1,70	0,51	875	65
I1	2,24	0,67	0	285
I2	2,13	0,64	150	265
I3	2,03	0,61	290	250
I4	1,56	0,47	875	235
J1	1,90	0,57	0	700
J2	1,80	0,54	150	670
J3	1,70	0,51	290	655
J4	1,25	0,37	875	615

For sample K general procedure was used with 140 mL of styrene, 42 mL of curing agent, 26.4 g of $BiPh_3$ 51.6 g of PPO and 192 mg of POPOP as well as 50 mg of AIBN as the initiator. Polymerization took place in a 40°C oven over a 25 days span.

For sample L general procedure was used with 150 mL of styrene, 45.2 mL of curing agent, 18.4 g of $Gd(TMHD)_3$, 5.5 g of PPO and 55 mg of bis-MSB as well as 10 mg of AIBN as the initiator. Polymerization took place in a 60°C oven over a 12 days span.

Acquisition set up

X-ray radiography was performed with a Yxlon™ Comet MXR-451 apparatus with tension set at 50 kV, recorded on a Kodak M-type argentic film.

Pulse height spectra were acquired using a Hamamatsu™ H1949-51 photocathode powered by an Ortec™ 556 High Voltage supply. Output signals were recorded unfiltered using a custom made acquisition setup.

Spectroscopy

Emission spectra were recorded using a Fluoromax 4P spectrofluorometer (Horiba) with excitation wavelength set at 380 nm.

Radioluminescence spectra were acquired by using the following procedure. In the Fluoromax 4P spectrofluorometer (Horiba), the excitation light was shut down. In the center of the experimenter chamber, $^{90}Sr/^{90}Y$ β-emitting source (25 MBq) was placed at 1 cm away from the scintillator to irradiate the plastic scintillator located close to the detection cell. Spectra were acquired with integration time 5 s/nm. Two types of blank spectra were recorded: one with the plastic scintillator without source and one with the source without scintillator, in order to establish a base line. Plastic scintillator EJ-200 was purchased from Eljen Technology and was used as reference set at 10,000 ph/MeV.

Lifetime spectra were recorded using the Time-Correlated Single Photon Counting (TCSPC) attachment on a Fluoromax 4P spectrofluorometer (Horiba). The pulsed nano-LED excitation wavelength was 270 nm and linked to a DeltaHub high throughput, synchronous detection block. Decay times were extracted using DAS-6 software.

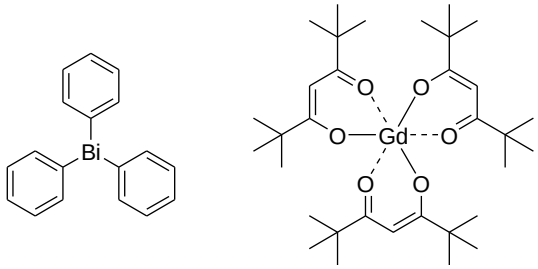

BiPh3 $Gd(TMHD)_3$

Scheme 1: formula of bismuth and gadolinium compounds used in this work

Results and discussion

Gadolinium is a major target for thermal neutron detection as it has a high thermal cross-section and does not need isotopic enrichment. Two of its natural occurring isotopes are ^{155}Gd (14.8%, 61 kbarn) and ^{157}Gd (15.7%, 254 kbarn). Based on previous work in the field of liquid scintillation and our previous work with organometallics, we decided to use $Gd(TMHD)_3$ (Scheme 1) as the metal source for loading the PS. A classic matrix was chosen based on previous good results, cheapness and scalability. It is composed of styrene, a curing agent, PPO and bis-MSB respectively primary and secondary fluorophores. The first results were encouraging, loading up to 3.6 % of metal was achieved (Figure 1). As expected scintillation yields decreased with higher loading, mainly because of the gadolinium and its heavy atom fluorescence quenching effect (FigSI1). The same phenomenon is observed for gadolinium and other elements such as tin[8], lead[12], and bismuth[24].

We decided to investigate this fluorescence quenching in order to find a way to minimize it. To understand the mechanism, two series of PS were synthesized, the first one explored bismuth loading, the second one gadolinium loading. General theory and previous work indicated that interaction between organometallic complexes and surrounding are crucial. At the end of the ionization cascade when excitation is just in the range of a few eV, Dexter and Förster transfers can occur between the organometallic compound and matrix components, mainly styrene and PPO. To probe those interactions, PPO concentration was also set as a variable in our bismuth and gadolinium screening (Figure 2).

For the Bismuth screening (A to E), metal loading up to 10 wt% was achieved with better optical characteristic than previously reported. For the gadolinium screening (F to J), we were able to reach a gadolinium content up to 5 wt%. We postulate that the heating step help solubilizing the $Gd(TMHD)_3$ by chelating the styrene, reaching hapticity superior to 6 which suits lanthanide better. In both screening PPO content steps (1 to 5) were set to be 0.5 wt% 1 wt% 3 wt% 9 wt% and 20 wt%. Samples were logically identified by a letter indicating its metal loading and a number indicating its PPO loading.

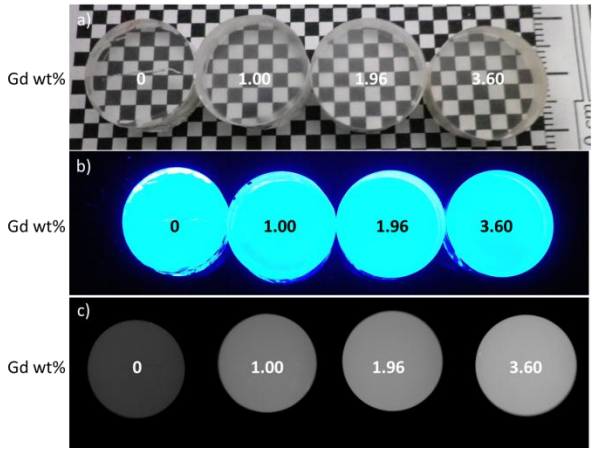

Figure 1: a) Photo of $Gd(TMHD)_3$ loaded scintillators. b) UV response of these scintillators. c) X-ray radiography snapshot showing homogeneity of the loading and increase attenuation power

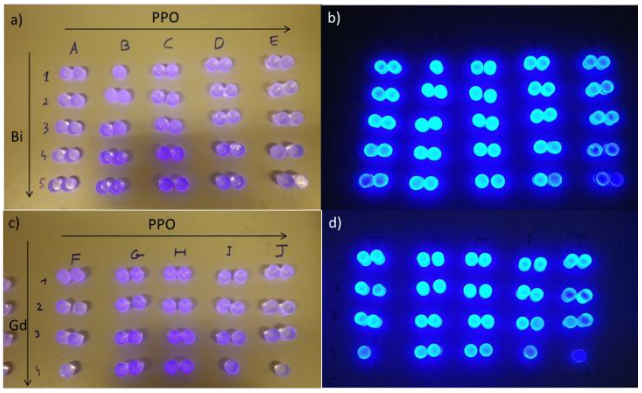

Figure 2: a) Snapshots of bismuth loaded plastic scintillator with various loading in $BiPh_3$ and PPO with UV illumination b) UV response of these scintillators in the dark. c) Photos of gadolinium loaded plastic scintillator with

various loading in $Gd(TMHD)_3$ and PPO. with UV illumination d) UV response of these scintillators in the dark. Each sample was doubled and had for dimension 1.6 cm^3 (h = 8 mm diam. = 16 mm)

Pulse height spectra were recorded for each sample with three different sources (^{241}Am (59 keV, 1 kBq), ^{137}Cs (662 keV, 200 kBq) and ^{22}Na (511 keV, 1275 keV, 20 MBq)), and their scintillation yields are given relative to the maximum. This maximum was compared to commercial EJ-200 PS and calibrated at 9900 $ph.MeV^{-1}$ (99% that of EJ-200). All results for the ^{137}Cs source are reported in Figure 3 and Figure 4. For a precise overview, scintillation yields are also reported in the ESI (tableSI1 and SI2).

As expected for both bismuth and gadolinium loadings, scintillation yields decreased while heavy metal concentration increased. This trend is steeper for the gadolinium, despite being lighter than bismuth, which is counterintuitive as the heavier the elements the more fluorescence get quenched. It confirmed that the surrounding of the metal have a major impact on the quenching mechanism. This phenomenon was approached in previous works but always put in balance with other effect cause by the ligand such as low solubility, degradation and/or auto adsorption.

The behavior in each series (Bi or Gd) was consistent for a wide range of energy from 59 keV (^{241}Am) to 1.28 MeV (^{22}Na) (figureSI2 to Si5). A most surprising fact appears when we compare those two series: there is a discrepancy in their general trend when PPO concentration is increasing.

For the bismuth loaded PS series (A to E), an increase of PPO concentration results in higher scintillation yield, the higher, the better. This is coherent with observation made on lead-loaded samples. Furthermore it indicates that increase of interactions between PPO and organo-bismuth is decreasing fluorescence quenching. We postulate that the aromatic moieties of the $BiPh_3$ complex act as antenna and favor Förster transfer with PPO. The fact that quenching tends to decrease with this can be explained by a majority of these transfers occurring from the $BiPh_3$ toward the PPO.

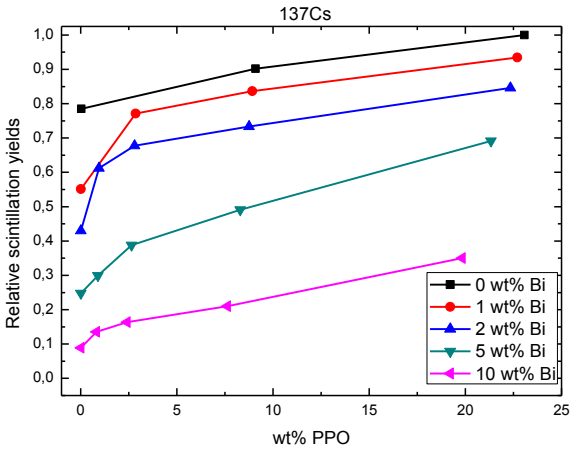

Figure 3: Evolution of scintillation yields with various PPO and bismuth concentration, series A to E.

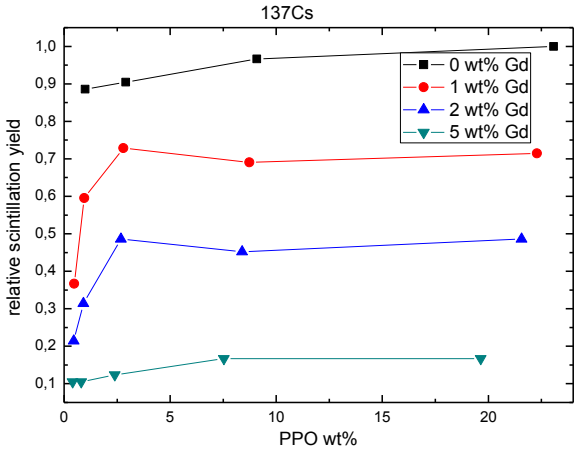

Figure 4: Evolution of scintillation yields with various PPO and gadolinium concentration, series F to J.

For the gadolinium series (F to J), a clear maximum of scintillation yield can be identified for PPO concentration around 3 wt%. This behavior is much closer to the non-loaded PS. It supports the fact that TMHD ligands act as an insulator layer between the metal and its surrounding, disabling possibility of exciton transfer.

To support our theory, experiments using triphenyl gadolinium or $Bi(TMHD)_3$ were tried, but scintillators loaded with these compound were very cloudy and not suitable for scintillation experiments.

The next step was to apply these conclusions to the fabrication of larger scintillator. Scale up can be very tricky but is a necessary step to demonstrate the feasibility. The goal here is to address two major challenges of the scintillation field: Gamma spectrometry with bismuth loaded PSs and thermal neutron detection with gadolinium loaded PSs.

For the realization of sample K, a loading of 5 wt% of Bismuth was chosen, as a compromised value between count rate increase and scintillation yield loss. A 155 cm^3, 187 g plastic scintillator was successfully synthesized (FigSI6). Lifetime, radioluminescence and emission spectra were obtained to fully characterize our bismuth loaded PS (Table 4) (FigSI7 to SI9). Pulse height spectra were recorded using different gamma sources. A photoelectric peak was successfully recorded for ^{57}Co (122 keV); this is coherent with previous result describing increase of PE event with an increase of Bi loading. Unfortunately only Compton edge was observed with a ^{137}Cs (662 keV, 200 kBq) source, which is in contradiction with the recent work of Cherepy *et al.*[25] Scintillator K was then compared with commercial 5 wt% lead loaded scintillator EJ-256-5 of equivalent volume (FigSI10 and SI11). Sample K's performances were found on par with EJ-256-5 in terms of total counting rate, photoelectric counting rate resolution and scintillation yields (Table 3).

Table 3: Comparison of main characteristic between commercial 5 wt% Pb loaded scintillator and sample K 5 wt% Bi loaded scintillators.

	^{57}Co (4 kBq)			^{137}Cs (200 kBq)	
	Scintillation yield (ph/MeV)	Total counting rate (cps)	PE counting rate (cps)	Scintillation yield (ph/MeV)	Total counting rate (cps)
EJ-256-5 wt% Pb	5200	705	245	5200	4500
K 5 wt% Bi	3900	710	330	4400	4400

Realization of high volume Gd-loaded PS was also successfully achieved with the fabrication of a cylindrical 97 cm^3, 108 g plastic scintillator (Figure 5) with 2 wt% of gadolinium. Characterization of this sample L showed a relative light yield of about 4200 ph.MeV^{-1}. Lifetime, emission and radioluminescence characterization were also performed and given in Table 4.

Evidences of gadolinium doped PS, for thermal neutron detection, are never straightforward. Multiple parameters must be considered to ensure that it is effectively thermal neutrons which are observed, as natural neutron sources are always gamma emitters too. A ^{252}Cf source was used in conjunction with lead/copper shielding and HDPE neutron thermalizer. The pulse height spectrum of L was compared with an unloaded PS equivalent in volume, density and yield (Figure 6). This comparison showed a dramatic count increase in the low energy part of the spectrum, consistent with gamma rays and internal conversion electrons resulting from neutron capture by a Gd nucleus. This *a minima* result is encouraging and researches are performed in our lab to exploit this work.

Table 4: Main characteristic of large volume scintillator K and L.

	Volume (cm^3)	Density	Scintillation yields (ph.MeV^{-1})	Emission λ_{max} (nm)	Decay time (ns)
K	155	1.21	4200*	438	1.98 ± 0.05
L	97	1.11	3000*	430	1.89 ± 0.01

* Mean value for three measurements at 59 keV, 122 keV and 662 keV

Conclusion.

This work used an iterative approach to optimize metal loading in PS. We showed that bismuth and gadolinium loadings do not behave in the same way and that it is easier to compensate for fluorescence quenching with bismuth. This effect was attributed to the ligand(s) surrounding the metal center. We found that the more interaction between the organometallic and the matrix, the better the light yields. Therefore aromatic organometallic compound should be privileged as opposed to isolate metal center from the matrix with aliphatic chains. We have also reported the fabrication of large scales Bi loaded plastic with performance on par with commercial lead loaded PS. And despite the strong fluorescence quenching we have demonstrated the ability of Gd(TMHD)$_3$ loaded PS to detect thermal neutron. Both applications gave us access to PS of significant volume (> 100 cm^3) that is necessary for field deployment.

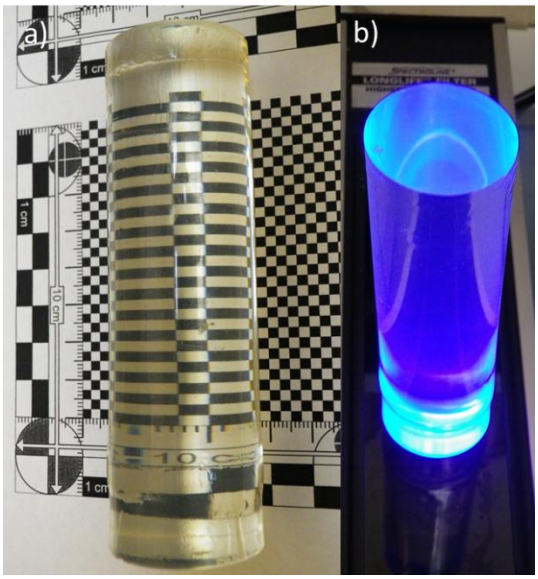

Figure 5: a) Photo of Gd(TMHD)$_3$ loaded scintillator. 97 cm^3, 108 g. b) UV response.

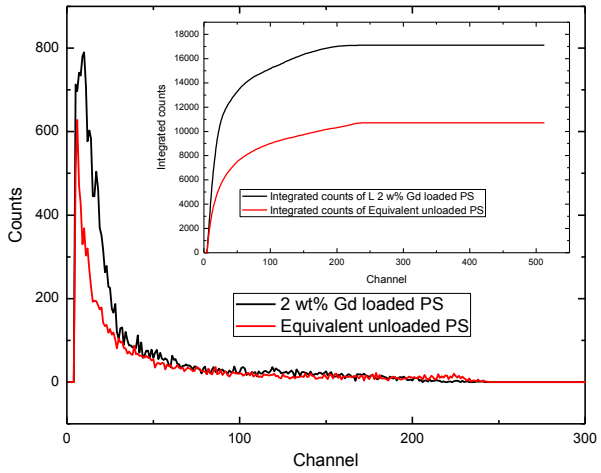

Figure 6: Pulse height spectra of a ^{252}Cf thermalized neutron/gamma source with a 2 wt% Gd loaded scintillator and its unloaded equivalent.

ASSOCIATED CONTENT

Complementary figures and tables are given in Supporting Information. This material is available free of charge via the Internet at http://pubs.acs.org.

AUTHOR INFORMATION

Corresponding Author

* Matthieu Hamel, Laboratoire Capteurs & Architectures Électroniques, DRT/LIST/DM2I/LCAE

CEA Saclay

91191 Gif Sur Yvette Cedex
Phone: +33 (0)169083325
email: matthieu.hamel@cea.fr (please do not send commercial emails)

Funding Sources

We thank the French "Direction Générale de l'Armement" and "Secrétariat Général de la Défense et de la Sécurité Nationale" for the grant associated to this project.

ACKNOWLEDGMENT

Bernard Rattoni is acknowledged for the x-ray radiography snapshot.

ABBREVIATIONS

CZT: Cadmium Zinc telluride

HPGe: High Purity Germanium

PS: Plastic scintillator

PPO: 2,5-diphenyloxazole

POPOP: 1,4-bis(5-phenyloxazol-2-yl)benzene

Bis-MSB: 1,4-Bis(2-methylstyryl)benzene

$Gd(TMHD)_3$: gadolinium tris-tetra-methyl-heptanedionate

$BiPh_3$: triphenyl bismuth

HDPE: high density poly ethylene

REFERENCES

(1) Bertrand, G. H. V.; Sguerra, F.; Hamel, M. *Chemistry - A European Journal* **2014**, *20*, 15660–15685.

(2) Knoll, G. F. In *Radiation detection and measurement*; 2000; p. 405.

(3) Knoll, G. F. In *Radiation detection and measurement*; 2000; p. 220.

(4) Bertrand, G. H. V.; Hamel, M.; Normand, S.; Sguerra, F. *Nuclear Instruments and Methods in Physics Research Section A: Accelerators, Spectrometers, Detectors and Associated Equipment* **2015**, *776*, 114–128.

(5) Rupert, B. L.; Cherepy, N. J.; Sturm, B. W.; Sanner, R. D.; Payne, S. A. *EPL (Europhysics Letters)* **2012**, *97*, 22002.

(6) Sguerra, F.; Marion, R.; Bertrand, G. H. V; Coulon, R.; Daniellou, R.; Gaillard, S.; Hamel, M. *Journal of Materials Chemistry C* **2014**, *2*, 6125–6133.

(7) Hamel, M.; Sibczynski, P.; Blanc, P.; Iwanowska, J.; Carrel, F.; Syntfeld-Kažuch, A.; Normand, S. *Nuclear Instruments and Methods in Physics Research Section A: Accelerators, Spectrometers, Detectors and Associated Equipment* **2014**, *768*, 26–31.

(8) Britvich, G. I.; Vasil'chenko, V. G.; Lapshin, V. G.; Solov'ev, A. S. *Instruments and Experimental Techniques* **2000**, *43*, 36–39.

(9) Hamel, M.; Normand, S.; Darbon, S.; Turk, G. French Patent Aplication FR2969169, 2012.

(10) Hamel, M.; Turk, G.; Simic, V.; Normand, S.; Darbon, S. *In LSC 2010, Advances in Liquid Scintillation Spectrometry* **2011**, 291–296.

(11) Hamel, M.; Normand, S.; Turk, G.; Darbon, S. *IEEE proceedings of ANIMMA 2011* **2012**.

(12) Hamel, M.; Turk, G.; Rousseau, A.; Darbon, S.; Reverdin, C.; Normand, S. *Nuclear Instruments and Methods in Physics Research Section A: Accelerators, Spectrometers, Detectors and Associated Equipment* **2011**, *660*, 57–63.

(13) Turk, G.; Reverdin, C.; Gontier, D.; Darbon, S.; Dujardin, C.; Ledoux, G.; Hamel, M.; Simic, V.; Normand, S. *The*

Review of scientific instruments **2010**, *81*, 10E509.

(14) Cherepy, N. J.; Sanner, R. D.; Tillotson, T. M.; Payne, S. A.; Beck, P. R.; Hunter, S.; Ahle, L.; Thelin, P. A. *2012 IEEE Nuclear Science Symposium and Medical Imaging Conference Record* **2012**, 1972–1973.

(15) Fritsch, J.; Mansfeld, D.; Mehring, M.; Wursche, R.; Grothe, J.; Kaskel, S. *Polymer* **2011**, *52*, 3263–3268.

(16) Negina, V. R.; Popov, V. N.; Nazarov, V. V *Pribory i Tekhnika Eksperimenta* **1980**, 60–62.

(17) Breukers, R. D.; Bartle, C. M.; Edgar, A. *Nuclear Instruments and Methods in Physics Research Section A: Accelerators, Spectrometers, Detectors and Associated Equipment* **2013**, *701*, 58–61.

(18) Normand, S.; Mouanda, B.; Haan, S.; Louvel, M. *Nuclear Instruments and Methods in Physics Research Section A: Accelerators, Spectrometers, Detectors and Associated Equipment* **2002**, *484*, 342–350.

(19) Britvich, G. I.; Vasil'chenko, V. G.; Gilitsky, Y. V.; Chubenko, A. P.; Kushnirenko, A. E.; Mamidzhanyan, E. A.; Pavluchenko, V. P.; Pikalov, V. A.; Romakhin, V. A.; Soldatov, A. P.; Sumaneev, O. V.; Chernichenko, S. K.; Shein, I. V.; Shepetov, A. L. *Nuclear Instruments and Methods in Physics Research Section A: Accelerators, Spectrometers, Detectors and Associated Equipment* **2005**, *550*, 343–358.

(20) Normand, S.; Delacour, P.; Passard, C.; Loridon, J. *IEEE Trans. Symp. Conf. Rec.* **2004**, *2*, 787–789.

(21) Bell, Z. W.; Miller, M. A.; Maya, L.; Brown, G. M.; Sloop, F. V. *IEEE Transactions on Nuclear Science* **2004**, *51*, 1773–1776.

(22) Bell, Z. W.; Brown, G. M.; Ho, C. H.; Sloop, F. V *Proceedings of SPIE* **2002**, *4784*, 150–163.

(23) Ovechkina, L.; Riley, K.; Miller, S.; Bell, Z.; Nagarkar, V. *Physics Procedia* **2009**, *2*, 161–170.

(24) Bertrand, G. H. V.; Sguerra, F.; Dehé-Pittance, C.; Carrel, F.; Coulon, R.; Normand, S.; Barat, E.; Dautremer, T.; Montagu, T.; Hamel, M. *Journal of Materials Chemistry C* **2014**, *2*, 7304–7312.

(25) Cherepy, N. J.; Sanner, R. D.; Beck, P. R.; Swanberg, E. L.; Tillotson, T. M.; Payne, S. A.; Hurlbut, C. R. *Nuclear Instruments and Methods in Physics Research Section A: Accelerators, Spectrometers, Detectors and Associated Equipment* **2015**, in press.

(26) Zaitseva, N.; Rupert, B. L.; PaweŁczak, I.; Glenn, A.; Martinez, H. P.; Carman, L.; Faust, M.; Cherepy, N.; Payne, S. *Nuclear Instruments and Methods in Physics Research Section A: Accelerators, Spectrometers, Detectors and Associated Equipment* **2012**, *668*, 88–93.

(27) Cai, W.; Chen, Q.; Cherepy, N.; Dooraghi, A.; Kishpaugh, D.; Chatziioannou, A.; Payne, S.; Xiang, W.; Pei, Q. *Journal of Materials Chemistry C* **2013**, *1*, 1970–1976.

Table of Contents artwork